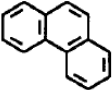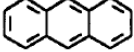# 11. Solubilities of Solids in Liquids

11.1 Thermodynamic Framework

Solubility depends not only on the activity coefficient of the solute but also on the fugacity of the standard state to which that activity coefficient refers and on the fugacity of the pure solid.

Table 11-1 Structures of phenanthrene and anthracene and their solubility in benzene at 25°C.

Solute	Structure	Solubility in benzene (mol %)
Phenanthrene		20.7
Anthracene		0.81

$$f_{2(pure\ solid)} = f_{2(solute\ in\ liquid\ solution)} \quad (11\text{-}1)$$

$$f_{2(pure\ solid)} = \gamma_2 x_2 f_2^0 \quad (11\text{-}2)$$

From eq. (11-2) the solubility is

$$x_2 = \frac{f_{2(pure\ solid)}}{\gamma_2 f_2^0} \quad (11\text{-}3)$$

Thus the solubility depends not only on the activity coeffcient but also on the ratio of two fugacities as indicated by Eq. (11-3).

To show the utility of Eq. (11-3), we consider first a very simple case.

1. Assume that the vapor pressures of the pure solid and of the subcooled liquid are not large.

-> In this case we can substitute vapor pressures for fugacities without serious error.

2. Assume that the chemical natures of the solvent and of the solute are similar.

In this case we can assume $\gamma_2 = 1$ and Eq. (11-3) becomes

$$x_2 = \frac{P^s_{2(pure\ solid)}}{P^s_{2(pure,\ subcooled\ liquid)}} \quad (11\text{-}4)$$

The solubility x_2 given by Eq. (11-4) is called the *ideal solubility*.

Equation (11-4) explains why phenanthrene and anthracene have very different solubilities in benzene. Because of structual differences, the triple-point temperatures of the two solids are significantly different. As a result, the pure-component fugacity ratios at the same temperature T also differ for the two solutes.
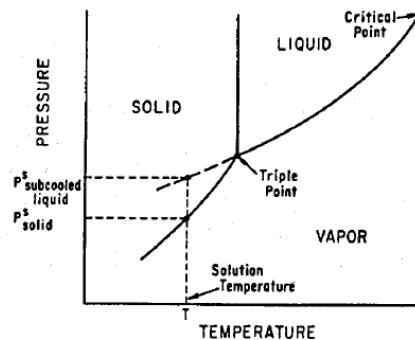
Figure 11-1   Extrapolation (dashed line) of liquid vapor pressure on a pressure-temperature diagram for a pure material (schematic).

The extrapolation indicated in Fig. 11-1 is simple when the solution temperature T is not far removed from the triple-point temperatrue. However, any essentially arbitrary extrapolation involves uncertainty; when the extrapolation is made over a wide temperature range, the uncertainty may be large.

11.2 Calculation of the Pure-Solute Fugacity Ratio

For the liquid-phase activity coefficient, we define the standard state as the pure, subcooled liquid at temperature T under its own saturation pressure.

Assuming negligible solubility of the solvent in the solid phase, $\square$, the equilibrium equation is

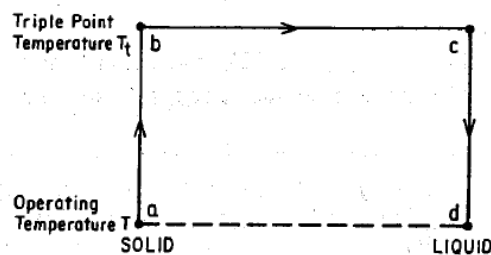$$x_2 = \frac{P_{2(pure\ solid)}}{\gamma_2 f_{2(pure,\ subcooled\ liquid)}} \quad (11\text{-}5)$$

To simplify notation, let

$$f_{2(pure\ solid)} = f_2^*$$

and let

$$f_{2(pure,\ subcooled\ liquid)} = f_2^L$$

These two fugacities depend only on the properties of the solute(component 2).

Figure 11-2 Thermodynamic cycle for calculating the fugacity of a pure subcooled liquid.

The ratio of these two fugacities can readily be calculated by the thermodynamic cycle indicated Fig. 11-2.

The molar Gibbs energy change for component 2 in going from a to d is related to the fugacities of solid and subcooled liquid by

$$\Delta g_{a \to d} = RT \ln \frac{f^L}{f^*} \quad (11\text{-}6)$$

where, for simplicity, subscript 2 has been omitted.

This Gibbs energy change is also related to the corresponding enthalpy and entropy changes by

$$\Delta g_{a \to d} = \Delta h_{a \to d} - T \Delta s_{a \to d} \quad (11\text{-}7)$$

The thermodynamic cycle in Fig. 11-2 provides a method to evaluate the enthalpy and entropy changes given in Eq. (11-7)

Because both enthalpy and entropy are state functions independent of the path, it is permissible to substitute for the path a→d the alternate path a→b→c→d. For the enthalpy change from a to d we have

$$\frac{\Delta h}{a \to d} = \frac{\Delta h}{a \to b} + \frac{\Delta h}{b \to c} + \frac{\Delta h}{c \to d} \quad (11\text{-}8)$$

Equation (11-8) can be rewritten in terms of heat capacity c_p and enthalpy of fusion $\Delta_{fus}h$

$$\frac{\Delta h}{a \to d} = \Delta_{fus}h_{at\ T_t} + \int_{T_t}^{T} \Delta c_p dT \quad (11\text{-}9)$$

where $\Delta c_p \equiv c_{p(liquid)} - c_{p(solid)}$ and T_t is the triple-point temperature.

Similarly, for the entropy change from a to d,

$$\frac{\Delta s}{a \to d} = \frac{\Delta s}{a \to b} + \frac{\Delta s}{b \to c} + \frac{\Delta s}{c \to d} \quad (11\text{-}10)$$

which becomes

$$\frac{\Delta s}{a \to d} = \Delta_{fus}s_{at\ T_t} + \int_{T_t}^{T} \frac{\Delta c_p}{T} dT \quad (11\text{-}11)$$

At the triple point, the entropy of fusion $\Delta_{fus}s$ is

$$\Delta_{fus}s = \frac{\Delta_{fus}h}{T_t} \quad (11\text{-}12)$$

Substituting Eqs. (11-7), (11-9), (11-11), and (11-12) into Eq. (11-6) , and assuming that Δc_p is constant over the temperature range $T \to T_t$, we obtain

$$\ln\frac{f^L}{f^s} = \frac{\Delta_{fus}h}{RT_t}\left(\frac{T_t}{T} - 1\right) - \frac{\Delta c_p}{R}\left(\frac{T_t}{T} - 1\right) + \frac{\Delta c_p}{R}\ln\frac{T_t}{T} \quad (11\text{-}13)$$

Equation (11-13) gives the desired result; it expresses the fugacity of the subcooled liquid at temperature T in terms of measurable thermodynamic properties.
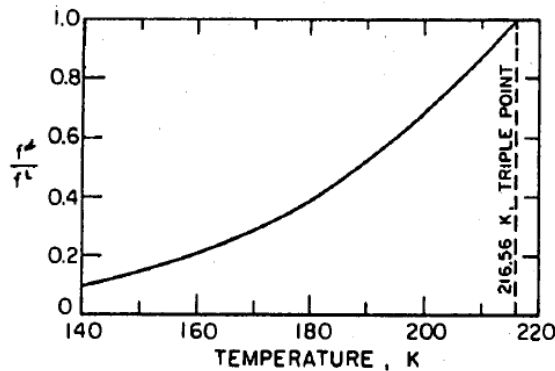

Figure 11-3 Fugacity ratio for solid and subcooled liquid carbon dioxide.

11.3 Ideal Solubility

An expression for the ideal solubility of a solid solute in a liquid solvent has already been given by Eq. (11-4), but no clear-cut method was given for the saturation pressure of the subcooled liquid.

However, this difficulty can be overcome by substituting Eq. (11-13) into Eq. (11-5).
If we assume that the solution is ideal, then $\gamma_2 = 1$ and we obtain for ideal solubility x_2.

$$\ln\frac{1}{x_2} = \frac{\Delta_{fus}h}{RT_t}\left(\frac{T_t}{T}-1\right) - \frac{\Delta c_p}{R}\left(\frac{T_t}{T}-1\right) + \frac{\Delta c_p}{R}\ln\frac{T_t}{T} \quad (11\text{-}14)$$

Equation (11-14) provides a reasonable method for estimating solubilities of solids in liquids where the chemical nature of the solute is similar to that of the solvent.

Equation (11-14) immediately leads to useful conclusions concerning the solubilities of solids in liquids.

●For a given solid/solvent system, the solubility increases with rising temperature. The rate of increase is approximately proportional to the enthalpy of fusion and, to a first approximation, does not depend on the melting temperature.

● For a given solvent and a fixed temperature, if two solids have similar enthalpies of fusion, the solid with the lower melting temperature has the higher solubility. Similarly, if the two solids have nearly the same melting temperature, the one with the lower enthalpy of fusion has the higher solubility.

To a fair approximation, the terms that include Δc_p in Eq. (11-14) may be neglected. Also, it is permissible to substitute melting temperatures for triple-point temperatures. Equation (11-14) may then be rewritten.

$$\ln x_2 = -\frac{\Delta_{fus} S}{R}\left(\frac{T_m}{T} - 1\right) \quad (11\text{-}15)$$
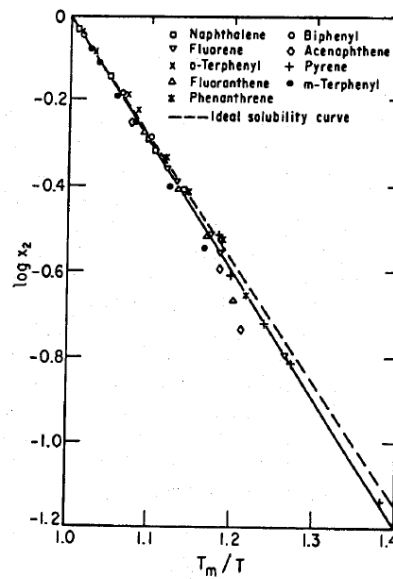
where T_m is the normal melting temperature.

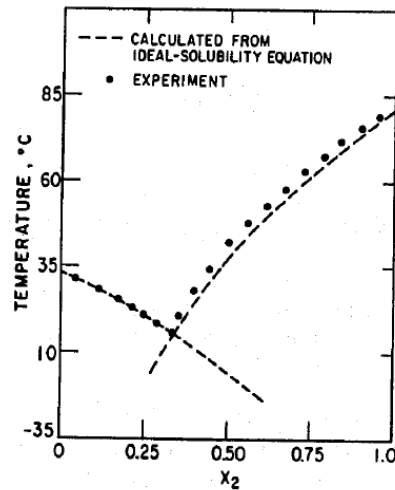**Figure 11-4** Solubility of aromatic solids in benzene.

Figure 11-5 Freezing points for the system *o*-chloronitrobenzene (1)/*p*-chloronitrobenzene (2).

11.4 Nonideal Solutions

Equation (11-14) assumes ideal behavior but Eqs. (11-5) and (11-13) are general. Whenever there is a significant difference in the nature and size of the solute and solvent molecules, we may expect that γ_2 is not equal to unity. In nonpolar solutions, where only dispersion forces are important, γ_2 is generally larger than unity (and thus the solubility is less than that corresponding to ideal behavior), but in cases where polar or specific chemical forces are important, the activity coefficients may well be less than unity with correspondingly higher solubilities.

As for solutions of liquid components, there is no general method for predicting activity coefficients of solid solutes in liquid solvents. For nonpolar solutes and solvents, however, a reasonable estimate can frequently be made with the Scatchard-Hildebrand relation

$$\ln\gamma_2 = \frac{v_2^l\left(\delta_1 - \delta_2\right)^2 \Phi_1^2}{RT} \quad (11\text{-}17)$$

where v_2^l is the molar volume of the subcooled liquid, δ_2 is the solubility parameter of the subcooled liquid, δ_1 is the solubility parameter of the solvent, and

$$\Phi_1 = \frac{x_1 v_1^l}{x_1 v_1^l + x_2 v_2^l}$$

is the volume fraction of the solvent.

Let $\Delta_{fus}v$ stand for the volume change of fusion at the triple-point temperature. That is,

$$\Delta_{fus}v = v_t^l - v_t^* \quad (11\text{-}18)$$

where subscript t refers to the triple-point temperature.

Let v^* be the molar volume of the solid at temperature T of the solution. The molar volume of the subcooled liquid is then given by

$$v^l = v^* + \Delta_{fus}v + (v_t^* \alpha_t^* - v_t^l \alpha^l)(T_t - T) \quad (11\text{-}19)$$

where α^* and α^l are the volumetric coefficients of expansion of the solid and liquid, respectively.

The energy of vaporization of the subcooled liquid is found in a similar manner. Let $\Delta_{fus}h$ stand for the enthalpy of fusion of the solid at the triple-point temperature and let $\Delta_{sub}h$ stand for the enthalpy of sublimation of the solid at temperature T. The energy of vaporization of the subcooled liquid is then

$$\Delta u = \Delta_{sub}h - \Delta_{fus}h + \Delta c_p(T_t - T) - P^s(v^G - v^l) \quad (11\text{-}20)$$

where P^s is the saturation pressure of the subcooled liquid and v^G is the molar volume of the saturated vapor in equilibrium with the solid, all at temperature T.

The square of the solubility parameter is defined as the ratio of the energy of complete vaporization to the liquid volume. Therefore, if the vapor pressure of the subcooled liquid is large, it is necessary to add a vapor-phase correction to the energy of vaporization given by Eq. (11-20). Such a correction, however, is rarely required and for most cases of interest the solubility parameter of the subcooled liquid is given with sufficient accuracy by

$$\delta_2 = \left(\frac{\Delta_{vap}u_2}{v_2^l} \right)^{1/2} \quad (11\text{-}21)$$

where $\Delta_{vap}u_2$ is the energy of vaporization, given by the enthalpy of vaporization minus RT.

As discussed in Chap. 7, the regular-solution theory of Scatchard-Hildebrand can be significantly improved when the geometric-mean assumption is not used. In that event, Eq. (11-17) becomes

$$\ln\gamma_2 = \frac{v_2^I\left[(\delta_1-\delta_2)^2+2l_{12}\delta_1\delta_2\right]\Phi_1^2}{RT} \quad (11\text{-}22)$$

The energy of vaporization was divided into two parts.

$$\Delta u = \Delta u_{disp} + \Delta u_{quad} \quad (11\text{-}23)$$

As a result, two cohesive-energy densities can now be computed, corresponding to the types of intermolecular forces:

$$c_{disp} \equiv \frac{\Delta u_{disp}}{v} \quad (11\text{-}24)$$

$$c_{quad} \equiv \frac{\Delta u_{quad}}{v} \quad (11\text{-}25)$$

where superscript L has been omitted.

The activity coefficient of component 2, the solute, dissolved in a nonpolar solvent, is now written

$$RT\ln\gamma_2 = v_2\Phi_1^2\left[c_1 + c_{2total} - 2(c_1 c_{2disp})^{1/2}\right] \quad (11\text{-}26)$$

where $c_{2total} = c_{2disp} + c_{2quad}.$

If $c_{2quad} = 0$, Eq. (11-26) reduces to Eq. (11-17).

To calculate the cohesive-energy density due to quadrupole forces, Myers derived the relation

$$c_{iquad} = \frac{\beta Q_i^4}{kT\left(\dfrac{v_i}{N_A}\right)^{13/3}} \quad (11\text{-}27)$$

where Q_i is the quadrapole moment of species i, v_i is the molar liquid volume, N_A is Avogadro's constant, k is Boltzmann's constant, T is the absolute temperature, and β is a dimensionless constant.

If the solvent, component 1, also has a significant quadrupole moment, then an additional term must be added to the bracketed quantity in Eq. (11-26) to account for quadrupole forces between the dissimilar components; further, the geometric-mean term must be modified to include only the dispersion cohesive –energy density of component 1. The bracketed term in Eq. (11-26) then becomes

$$\left[c_{1total} + c_{2total} - 2\left(c_{1disp} c_{2disp} \right)^{1/2} - 2c_{12quad} \right]$$

Using the theory of intermolecular forces, Myers showed that

$$c_{12quad} = \frac{\beta Q_1^2 Q_2^2}{kT \left(\frac{v_{12}}{N_A} \right)^{13/3}} \qquad (11\text{-}28)$$

where β is the same as in Eq. (11-27).

For v_{12} Myers used the combining rule

$$v_{12}^{1/3} = \frac{1}{2} \left(v_1^{1/3} + v_2^{1/3} \right) \qquad (11\text{-}29)$$

The term c_{12quad} is frequently negligible but it is important.

As Briefly indicated in Chap. 6, liquid-phase activity coefficients can sometimes be estimated from a group-contribution method such as UNIFAC.

In the liquid phase, it is also possible to calculate the fugacity of the dissolved component using an equation of state. For solute 2, the equation of equilibrium is written

$$f_2^* = \phi_2 x_2 P \qquad (11\text{-}30)$$

where ϕ_2 is obtained from an equation of state, valid for the fluid mixture, over the density range from zero density to liquid density, as discussed in Chaps. 3 and 12.

From experimental solid-liquid equilibrium (SLE) data we can obtain the binary parameters of a particular liquid-phase activity coefficient model, such as Wilson or UNIQUAC. These parameters may give in turn liquid phase activity coefficients at different system conditions that can be used to predict other equilibria.

11.5 Solubility of a Solid in Mixed Solvent

Scatchard-Hildebrand theory predicts that the solubility of a solid is a maximum in that solvent whose solubility parameter is the same as that of the (liquid) solute. In that event, the activity coefficient of the solute is equal to unity. Scatchard-Hildebrand theory suggests, therefore, that when a solid solute is dissolved in a mixture of two carefully selected solvents, a plot of solubility versus solvent composition should go through a maximum. : *maximum-solubility effect*
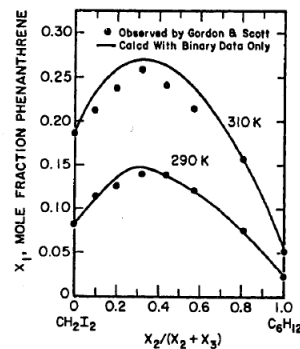
Figure 11-13 Solubility of phenanthrene in a mixed solvent containing cyclohexane and methylene iodide.

Shown in Fig. 11-13 are calculations based on regular-solution theory without, however, using the geometric-mean assumption. The activity coefficient is given by

$$\ln \gamma_1 = \frac{v_1}{RT}\left[A_{12}\Phi_2^2 + A_{13}\Phi_3^2 + (A_{12} + A_{13} - A_{23})\Phi_2\Phi_3 \right] \quad (11\text{-}31)$$

where

$$A_{ij} = (\delta_i - \delta_j)^2 + 2l_{ij}\delta_i\delta_j$$

Parameters l_{ij}, that give deviations from the geometric mean, are obtained from binary data reported by Gordon and Scott. For the two binaries including phenanthrene, l_{12} and l_{13} are obtained from experimental solubilities of phenanthrene in each of the two solvents at 25°C. In these calculations, all parameters were taken as independent of temperature.

A group-contribution method such as UNIFAC may sometimes be used to calculate liquid-phase activity coefficients of solutes in mixed solvents.

| Alcohol	Mole fraction alcohol in solvent mixture[†]	Temp. (°C)	Solubility (mol %)		
			Ideal	UNIFAC	Exp.*
Methanol	0.922	35.7	39.7	2.8	2.4
	0.922	50.6	55.8	4.8	4.6
Ethanol	0.906	27.5	32.7	2.6	3.4
	0.906	39.5	43.5	3.8	5.5
	0.743	73.0	47.0	2.0	3.8
1-Propanol	0.739	40.9	44.9	3.7	5.6
	0.739	46.7	51.4	4.4	7.4
	0.616	52.1	57.6	3.0	5.7
1-Butanol	0.813	21.8	28.3	3.5	4.3
	0.813	29.6	34.1	4.6	5.8
	0.680	30.7	35.3	2.9	4.7
	0.680	43.5	47.7	4.5	8.0

Table 11-2 gives calculated and experimental solubilities for naphthalene in aqueous solvents containing methanol, ethanol, propanol, or butanol. The ideal solubilities ($\gamma_2 = 1$) are always too large by one order of magnitude. Solubilities calculated with UNIFAC are in semiquantitative agreement with experiment.

For a solid dissolved in a binary mixed solvent, *enhanced solubility* (or maximum-solubility effect) has been observed for a large variety of systems.

(1)

$t_m = 98.60°C$

$\Delta_{fus}h = 22.52 \text{ kJ mol}^{-1}$

(2)

$t_m = 63.75°C$

$\Delta_{fus}h = 21.34 \text{ kJ mol}^{-1}$
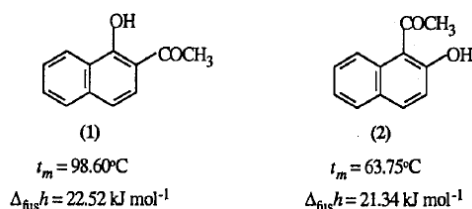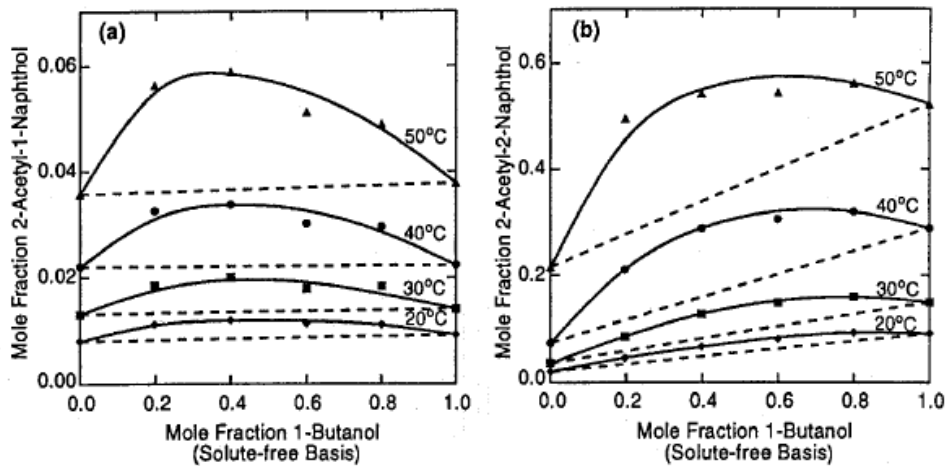
Figure 11-14 Solubility isotherms for (a) 2-acetyl-1-naphthol (1) and (b) 1-acetyl-2-naphthol (2) in cyclohexane/1-butanol mixed solvent system (Domanska, 1990). ⎯⎯⎯ Smoothed experimental data (symbols); – – – Additivity rule.
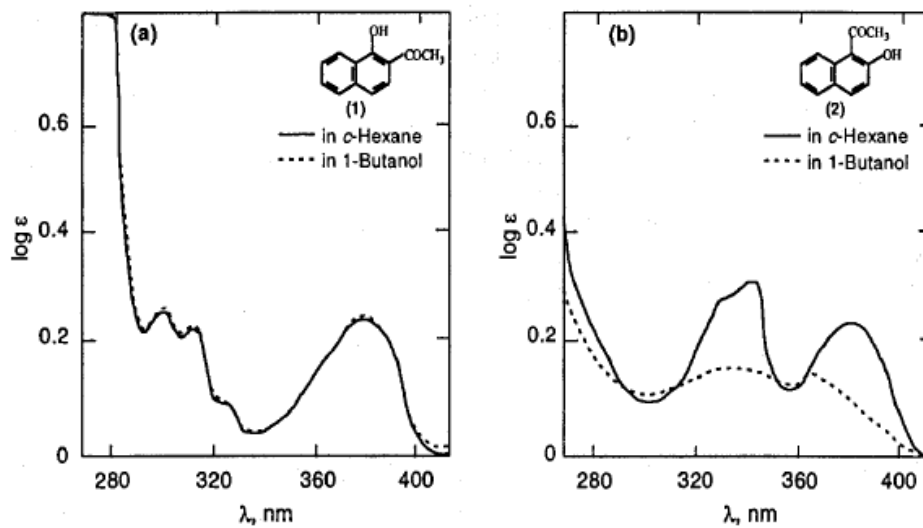
Figure 11-15 Schematics of ultraviolet absorption spectra for (a) 2-acetyl-1-naphthol (1) and (b) 1-acetyl-2-naphthol (2), in cyclohexane (⎯⎯⎯) and in 1-butanol (- - - -). Here ε is the extinction coefficient.

11.6 Solid Solutions

There are many situations where components 1 and 2 are miscible not only in the liquid phase but in the solid phase as well. In such cases we must write two equations of equilibrium, one for each component.

$$f_{1(solid\ phase)} = f_{1(liquid\ phase)} \quad (11\text{-}32)$$

$$f_{2(solid\,phase)} = f_{2(liquid\,phase)} \quad (11\text{-}33)$$

Introducing activity coefficients we can rewrite these equations.

$$\gamma_1^* x_1^* f_{pure1}^* = \gamma_1^L x_1^L f_{pure1}^L \quad (11\text{-}34)$$

$$\gamma_2^* x_2^* f_{pure2}^* = \gamma_2^L x_2^L f_{pure2}^L \quad (11\text{-}35)$$

If system temperature T is above the triple-point temperature of component 1 but below that of component 2, then pure solid 1 and pure liquid 2 are both hypothetical.

When Eqs. (11-34) and (11-35) are applied over a range of temperatures, it is possible to calculate the freezing-point diagram for the binary system.
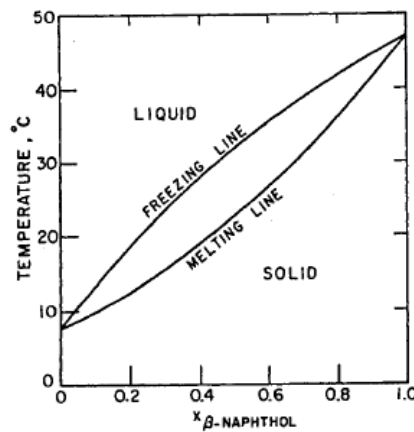
Figure 11-17 Phase diagram for the system naphthalene/β-naphthol.

It is difficult to say a priori whether or not two components are partially or totally miscible in the solide phase. For nonpolar substances the general rule is that solid-phase miscibility is usually negligible provided that the two components differ appreciably in molecular size and shape.

Because our knowledge of solid-phase mixtures is so meager, in many typical chemical-engineering calculations for multicomponent systems, it has been customary to assume either that there is complete immiscibility or (more rarely) complete miscibility in the solid phase.

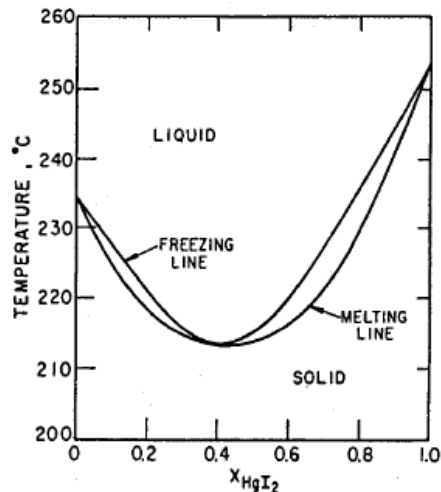Unfortunately, calculated phase equilibria are extremely sensitive to this choice of assumption.

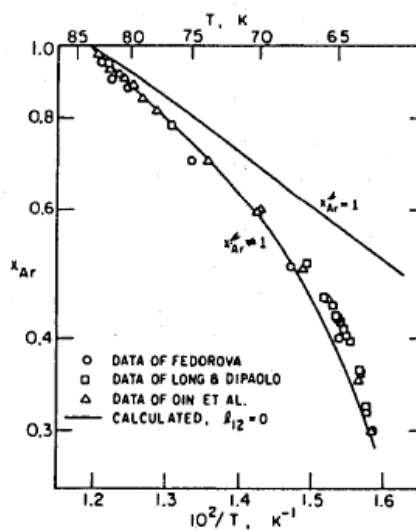**Figure 11-18** Phase diagram for the system HgBr$_2$/HgI$_2$.

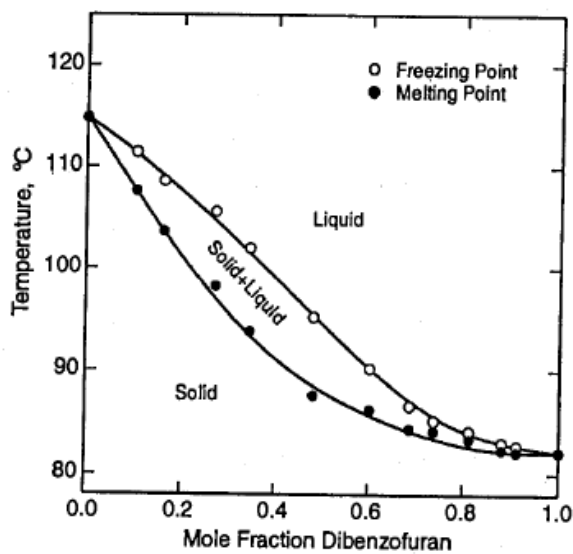**Figure 11-19** Solubility of argon in nitrogen.

Figure 11-20 Experimental solid-liquid phase diagram for the system fluorene/dibenzofuran (Sediawan *et al.*, 1989). ——— Smoothed data.
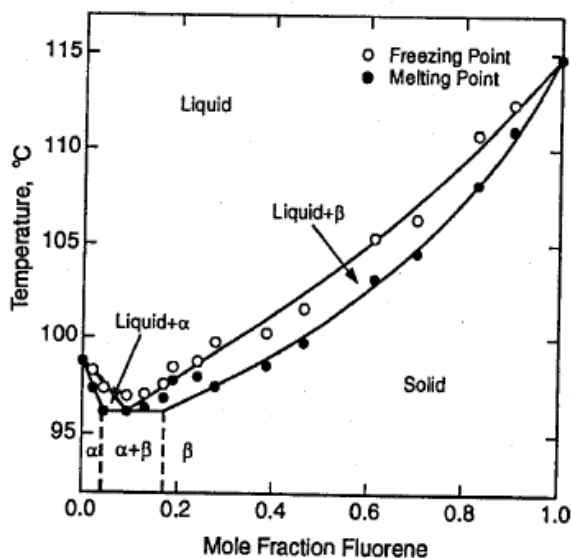

Figure 11-21 Experimental solid-liquid phase diagram for the system fluorene/dibenzothiophene (Sediawan *et al.*, 1989). ——— Smoothed data.

11.7 Solubility of Antibiotics in Mixed Nonaqueous Solvents

An industrial application that requires solid-liquid equilibria is provided by separation and recovery processes for amino acids and antibiotics. A simple solubility model for amino acids and antibiotics was presented by Gupta and Heidemann using a modified UNIFAC equation.

Using available experimental solubilities of the antibiotic in different solvents, and considering the entire antibiotic molecule as a group, Gupta and Heidemann wanted to obtain UNIFAC group-interaction parameters. To do so, they obtained from experimental solubility data the activity coefficient of the solid at saturation, using an equation similar to Eq. (11-15)

$$\gamma_2^{sat} = \frac{1}{x_2^{sat}} exp\left[-\frac{\Delta_{fus}S}{R}\left(\frac{T_m}{T}-1\right)\right] \quad \text{(11-36)}$$
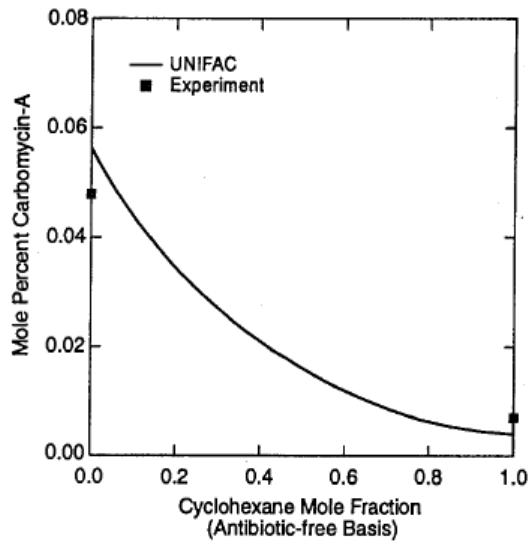
Figure 11-22 Solubility of carbomycin-A in mixtures of toluene and cyclohexane at 28°C. —— UNIFAC; ■ Experiment.
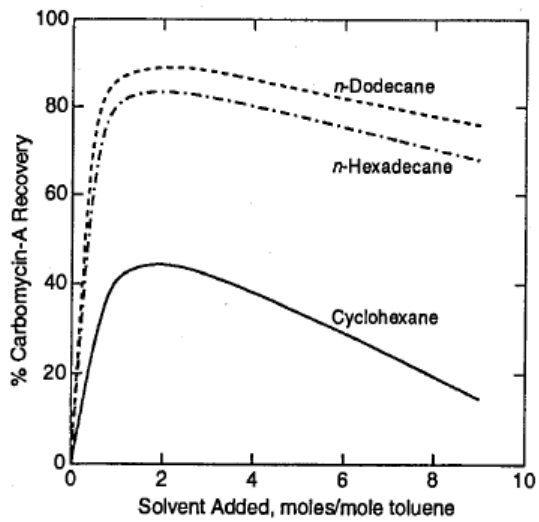

Figure 11-23 Predicted (from UNIFAC) recovery of carbomycin-A from saturated solutions in toluene upon dilution with a selected hydrocarbon.